Recursive simulation of quantum annealing and signatures of quantum behavior

A P Sowa[1], M J Everitt[2], J H Samson[2], S.E. Savel'ev[2], A M Zagoskin[2]
[1] *University of Saskatchewan and*
[2] *Department of Physics, Loughborough University, Loughborough, Leics LE11 3TU, UK*
(Dated: July 2, 2014)

The evaluation of the performance of adiabatic annealers is hindered by lack of efficient algorithms for simulating their behavior. We exploit the analyticity of the standard model for the adiabatic quantum process to develop an efficient recursive method for its numerical simulation in case of both unitary and non-unitary evolution. Numerical simulations show distinctly different distributions for the most important figure of merit of adiabatic quantum computing — the success probability — in these two cases. Our findings bear on the recent experimental results on controlled quantum annealing in the D-Wave One device [1] and indicate that they could be explained by quantum evolution in the presence of unexpectedly weak decoherence.

I. INTRODUCTION

The ongoing debate whether the devices D-Wave One and D-Wave Two, which contain hundreds of superconducting flux qubits, demonstrate quantum or classical annealing [1–6], is to a large extent due to the fact that their quantitative simulation is at the moment impossible. Characteristically, there was no controversy over quantum behaviour of an 8-qubit register [7], where a quantitative agreement was found between the experimental data and the theoretical predictions. Though one cannot expect to be able to model classically a large enough quantum system [8], the development of efficient classical algorithms could hopefully enable us to model quantum systems just big enough to take over. We can also exploit the idiosyncratic features of certain quantum devices, which simplify their modeling by classical means. Here we demonstrate such an algorithm for modeling linear adiabatic evolution, including the case when decoherence is present. This result depends on the analyticity of the final state of the system as a function of evolution time, which is rigorously proven. Comparing our small-scale numerical realizations of this algorithm, we find some indications that D-Wave machines might actually manifest quantum behavior.

An adiabatic process evolves the state vector of a quantum annealer over time T along the trajectory $s \mapsto |\psi(s)\rangle$, where the parameter $s \in [0,1]$ is the reduced time $s = t/T$. The initial value $|\psi(0)\rangle$ is the ground state of the initial Hamiltonian H_i. When the process stops at $t = T$ the state $|\psi(1)\rangle$ is considered as an approximant to the ground state of the custom design Hamiltonian H_f, which encodes the solution of an optimization problem of choice. We consider the standard linear case, when the evolution is driven by the time-dependent Hamiltonian

$$H(s) = (1-s)H_i + sH_f, \tag{1}$$

according to the Schrödinger equation

$$\frac{d}{ds}|\psi(s)\rangle = -i(T/\hbar)\, H(s)\, |\psi(s)\rangle. \tag{2}$$

Let the quantum system be an N-qubit register. In order to fix notation we describe the eigenstates and the corresponding eigenvalues of $H(s)$:

$$H(s)\,|m;s\rangle = E_m(s)\,|m;s\rangle, \quad \text{where} \;\; E_0(s) \le E_1(s) \le \ldots \le E_{2^N-1}(s). \tag{3}$$

However, this assumption is not necessary to derive the analytic results presented in next section. As we will see, our analysis remains valid in every case of bounded (in particular, finite) Hamiltonians H_i, H_f.

The purpose of analysis and simulation of (1) is estimation of the success probability

$$P = |\langle\psi(1)|0;1\rangle|^2, \tag{4}$$

which provides a measure of the accuracy with which the adiabatic process finds the solution of the underlying problem.

Having fixed T and the number of steps and the Hamiltonian, we repeatedly conduct the numerical experiment. Final Hamiltonians are drawn from an ensemble of binary optimization problems and the simulation outputs the

probability of success P for each instance of H_f. We record the outcome of the series of experiments in a histogram of P values. This type of data is comparable to the outcome of experiments with D-Wave One reported in [1]. The histogram of the probability of success has long been adopted as a means for testing hypotheses about adiabatic computing, see e.g. [9].

II. CONSEQUENCES OF ANALYTICITY

Since Hamiltonian (1) depends on parameter s linearly, the solution of Eq. (2) may be expected to depend on s analytically, at least for small s. Thus, we look for solutions in the form of a Taylor series

$$\psi(s) = \psi_0 + s\psi_1 + s^2\psi_2 + s^3\psi_3 + \dots \tag{5}$$

In order to simplify notation, let us define auxiliary operators

$$A = -i(T/\hbar)\, H_i \quad \text{and} \quad B = -i(T/\hbar)\,(H_f - H_i). \tag{6}$$

Thus, (2) is equivalent to

$$\frac{d}{ds}|\psi(s)\rangle = (A + Bs)\,|\psi(s)\rangle. \tag{7}$$

Below we will consider this equation for general bounded operators A and B, and only later draw conclusions about the specific case (6) relevant to the application at hand.

Substituting (5) in (7) we readily obtain

$$\begin{array}{rcl} |\psi_0\rangle &=& |\psi(0)\rangle \\ |\psi_1\rangle &=& A\,|\psi_0\rangle \\ \vdots & & \\ |\psi_n\rangle &=& \frac{1}{n}\,(A\,|\psi_{n-1}\rangle + B\,|\psi_{n-2}\rangle) \qquad \text{for } n \geq 2 \end{array} \tag{8}$$

We use this recurrence as the core of numerical schemas for simulation of the solutions of (1). It allows relatively efficient, as compared to ODE simulation, computation of consecutive terms and consecutive partial sums of the series (5). (Numerical experiment shows that this method is typically faster than the standard ODE solver such as the MATLAB's 'ode45' by a factor exceeding 3 for $N \leq 12$ qubits. For $N = 14$, in which case the memory constraint plays a significant role, the speed up factor is approximately 60, reducing the computation time from just under one hour to under one minute.) Note that evaluation of the success probability (4) requires only the computation of

$$P = |\langle\psi_0|0;1\rangle + \langle\psi_1|0;1\rangle + \langle\psi_2|0;1\rangle + \dots|^2.$$

In other words, the solution is found, immediately as it were, at the point $s = 1$ without the need of finding all the intermediate states $|\psi(s)\rangle$. This is in stark contrast to the computation based on an application of an ODE solver to Eq. (2). The current method has been tested against our earlier study of the correlation between gap and success probability[10]; in that work we used a conventional (Dormand-Prince) solver. Note also that if series (5) is known to converge absolutely, then $|\psi(s)\rangle$ automatically satisfies (2). Therefore, the main issue at stake is the estimation of the radius of convergence

$$R_c = \left(\limsup_{n\to\infty} \|\psi_n\|^{1/n}\right)^{-1}. \tag{9}$$

Here $\|\,\|$ denotes the ℓ_2 norm. In general R_c depends on the constituents of the process H_i, H_f and possibly even $|\psi(0)\rangle$. From the point of view of simulations it is ideal to have $R_c = \infty$, which ensures that $|\psi(s)\rangle$ given in (5) is the solution of (2) for all (reduced) times s. If on the other hand, $R_c < 1$, then the series cannot be used to estimate the success probability. But, as we shall see, the series (5) converges everywhere.

Let us introduce the following notation:

$$a := \|A\|, \quad b := \|B\|. \tag{10}$$

Here, $\|\,\|$ is the operator norm. Throughout the article we assume $0 < a, b < \infty$. For the particular case of (6), we have $a = (T/\hbar)\,\|H_i\|$, $\quad b = (T/\hbar)\,\|H_i - H_f\|$. The Hamiltonians are nontrivial and bounded, e.g. finite dimensional, and, moreover, $H_i \neq H_f$. We have the following result (see Supporting materials for the proof):

Theorem II.1. *$R_c = \infty$, i.e. series (5) converges absolutely in the entire complex plane and its limit $\psi(s)$ for $s \in [0, \infty)$ is the solution of (7) satisfying the initial condition $\psi(0) = \psi_0$.*

III. THE MASTER EQUATION

Now we will extend the above results to the evolution described by the master equation (see e.g. [11]):

$$\frac{d}{dt}\,\rho = -\frac{i}{\hbar}[H,\rho] + L\rho L^\dagger - \frac{1}{2}L^\dagger L\rho - \frac{1}{2}\rho L^\dagger L.$$

Here, ρ is the density matrix, H is the quantum system Hamiltonian and the Lindblad operator L accounts for decoherence due to the uncontrollable interaction of the quantum system with the environment. In some applications the master equation involves a finite number of different Lindblad operators. While for our purposes it is sufficient to have just one Lindblad, the results presented here can easily be extended to the more general case. From now on we will only consider the evolution of finite-dimensional systems. Furthermore, as before we assume that H takes the special form (1) with $s = t/T$. Substituting variables (6) as before, we obtain an equivalent form of the master equation

$$\frac{d}{ds}\,\rho = \mathcal{L}_A[\rho] + s\mathcal{L}_B[\rho] \tag{11}$$

with the shorthand notation

$$\mathcal{L}_A[\rho] := [A,\rho] + T\left(L\rho L^\dagger - \frac{1}{2}L^\dagger L\rho - \frac{1}{2}\rho L^\dagger L\right), \quad \text{and} \quad \mathcal{L}_B[\rho] := [B,\rho]. \tag{12}$$

Note that the evolution equation (11) generalizes the von Neumann equation

$$\frac{d}{ds}\rho(s) = -i(T/\hbar)\;[H(s),\rho(s)]. \tag{13}$$

In the context of adiabatic computing, it is vital to realize that there is an essential difference between the two types of evolution. Namely, at least if certain general conditions on H_f are satisfied, the adiabatic theorem applies to the case (13) and ensures that the probability of success increases with increasing T and will tend to one as T tends to infinity. In contrast, there is no known generalization of the adiabatic theorem, extending it to the case of (11). In fact, in the course of numerical experimentations we have observed that for a relatively large L the probability of success may decrease with increasing time T. Figure 7 illustrates this phenomenon. This observation agrees with the conclusions of Ref. [12] that there is a finite time window for the operation of a quantum annealer interacting with the thermal bath.

In order to describe the analytic properties of (11) we introduce the Hilbert space structure on the linear space of $K \times K$ matrices (e.g. $K = 2^N$ for an N qubit system). For $X \in \mathbb{C}^{K\times K}$ we define the Hilbert-Schmidt norm $\|X\|_{HS} = \mathrm{Tr}\,(XX^\dagger)^{1/2}$. This norm endows $\mathbb{C}^{K\times K}$ with the Hilbert space structure. We denote the corresponding operator norms of $\mathcal{L}_A, \mathcal{L}_B : \mathbb{C}^{K\times K} \to \mathbb{C}^{K\times K}$ simply by $\|\mathcal{L}_A\|, \|\mathcal{L}_B\|$. As is well known, the Hilbert-Schmidt norm has the submultiplicative property $\|AB\|_{HS} \le \|A\|_{HS}\,\|B\|_{HS}$ which, when applied to (12), yields the following estimates:

$$\|\mathcal{L}_A\| \le 2\|A\|_{HS} + 2T\,\|L\|_{HS}^2, \quad \|\mathcal{L}_B\| \le 2\|B\|_{HS}. \tag{14}$$

Next, we wish to consider solutions of (11). To this end we introduce the Taylor series Ansatz

$$\rho(s) = \rho_0 + s\rho_1 + s^2\rho_2 + s^3\rho_3 + \ldots \tag{15}$$

As before, we substitute (15) into (11). In this way we obtain the following description of the Taylor series coefficients:

$$\rho_n = \frac{1}{n!}\,Q_n(\mathcal{L}_A,\mathcal{L}_B)\rho_0, \tag{16}$$

where $Q_n = Q_n(\mathcal{L}_A, \mathcal{L}_B)$ is a polynomial in variables $\mathcal{L}_A$ and $\mathcal{L}_B$ defined by recursion:

$$\begin{array}{rcl} Q_0 & = & I \\ Q_1 & = & \mathcal{L}_A \\ \vdots & & \\ Q_{n+1} & = & \mathcal{L}_A Q_n + n\mathcal{L}_B Q_{n-1} \quad \text{for } n \geq 1. \end{array} \tag{17}$$

We observe that the proof of Theorem 1 (see Supporting materials) can be repeated almost verbatim with obvious modifications such as: replacing $A \rightsquigarrow \mathcal{L}_A$, $B \rightsquigarrow \mathcal{L}_B$, $P_n \rightsquigarrow Q_n$, and redefining $a := \|\mathcal{L}_A\|$ and $b := \|\mathcal{L}_B\|$. This yields the following result:

Theorem III.1. *Series (15) with coefficients defined via (16) and (17) converges absolutely in the entire complex plane. Moreover, its limit $\rho(s)$ for $s \in [0, \infty)$ is the solution of (11) satisfying the initial condition $\rho(0) = \rho_0$.*

IV. NUMERICAL EXPERIMENTS

We have conducted numerical experiments for both a pure adiabatic process (2) and the process with dissipation (11). With N qubits we use the following Hamiltonians:

$$H_i = -\sum_k \sigma_k^x, \quad k \in 1, 2, \ldots, N, \tag{18}$$

$$H_f = H_{\text{Ising}} = -\sum_{k<l} J_{kl}\, \sigma_k^z \sigma_l^z, \quad k, l \in 1, 2, \ldots, N. \tag{19}$$

Here, $J_{ij} \in \{-1, 1\}$ denote random variables with uniform distribution $P(J_{ij} = 1) = P(J_{ij} = -1) = 1/2$. In numerical experiments the choice of values for J_{ij}'s is generated via MATLAB's generic random number generators. It is done independently for every run of the experiments discussed below. Note that $\|H_i\| = N$ and $|H_f\| \leq N(N-1)/2$.

While Theorems II.1 and III.1 ensure that the Taylor series defining solutions of Eqns. (7) and (11) converge in the entire complex plane, numerical practice is more complicated. Namely, due to the roundoff error the Taylor series need not converge for relatively large values of T as intermediate sums become exponentially large in the adiabatic regime. The largest term $x^n/n!$ in the Taylor expansion of e^x occurs when $n \approx |x|$ and is of the order of $e^{|x|}$. However, we are frequently still able to obtain solutions in such cases using the following observation. Defining $\tau = s - s_0$ we observe that $\psi(\tau)$ satisfies (7) where s has been replaced by τ and A replaced by $A + s_0 B$ with the initial condition $\psi|_{\tau=0} = \psi(s_0)$. Similarly, $\rho(\tau)$ satisfies (11) where s has been replaced by τ and A replaced by $A + s_0 B$ with the initial condition $\rho|_{\tau=0} = \rho(s_0)$. This enables one to conduct computation in stages by partitioning the s-interval $[0, 1]$ into smaller segments. Since computation within each segment is based on a faster converging Taylor series we obtain convergence of the solution in the entire s-interval for larger values of T. Even though convergence in each subinterval is faster, the computational time is generally increased by a constant factor not exceeding the number of stages.

A. Unitary adiabatic evolution: Schrödinger's equation

We use a schema based on recurrence (8). Furthermore, we set $|\psi_0\rangle$ to be the ground state of H_i. We note that H_f is exponentially degenerate: the Hilbert space is 2^N-dimensional but there are only $O(N)$ distinct eigenvalues, which are separated by multiples of 2. In particular, the Hamiltonian $H(s)$ is invariant under a global spin flip for all time, so adiabatic evolution occurs in the subspace spanned by equal superpositions of computational states and the corresponding spin-flipped states, $\left\{\left(|abc\cdots\rangle + |\bar{a}\bar{b}\bar{c}\cdots\rangle\right)/\sqrt{2}\right\}$. Let Π denote the projector onto the ground state space of H_f. The probability of success is defined as $P = \|\Pi\psi(1)\|^2$. Note that even though the theoretical solution described in Theorem II.1 is guaranteed to exist for all s in practice the partial sum of the Taylor series may be irreparably deformed by the round off error before convergence happens. Thus, in a very small percentage of cases the algorithm in its typical setting does not converge and fails to produce a solution.

The results from simulation are presented via probability of success histograms, Fig. 1, and Figs. 3–6. Of note is the ragged landscape feature of the histogram for an 8 qubit system, Fig. 1. This can be understood qualitatively in the following way. The success probability is largely determined by the low-lying eigenvalue structure.

The aforementioned degeneracy reduces the number of qualitatively different classes and we conjecture that the peaks correspond to different classes. The ragged landscape is less apparent for larger systems. However, a new phenomenon emerges for systems as large as 12 qubits. Namely, the isolated islands (clusters) of probability of success concentrating in an infinitesimal neighborhood of 0, see Figs. 5, 6. We believe the latter phenomenon is due to the existence of optimization problems that are inherently hard. Since the optimization problem at hand is known to be NP hard, [13], we expect this phenomenon to persist for larger systems. Unfortunately, systems larger than 12 qubits are essentially out of reach, which is mostly due to limitations on memory capacity of a classical digital computer rather than the speed of computation. Finally, we emphasize that classical simulation of quantum annealing is still a classical algorithm, and no conclusions can be drawn at the moment as to whether or not the hard cases can be addressed with more effectiveness by a truly quantum process.

B. Non-unitary adiabatic evolution: Master equation with one Lindblad operator

We use a schema based on recurrence (in notation of Subsection III):

$$\begin{array}{lcl} \rho_0 & = & |\psi_0\rangle\langle\psi_0|, \quad \text{where } \psi_0 \text{ denotes the ground state of } H_i \\ \rho_1 & = & \mathcal{L}_A\rho_0 \\ \vdots & & \\ \rho_{n+1} & = & \frac{1}{n+1}\mathcal{L}_A\left(\rho_n + \mathcal{L}_B\rho_{n-1}\right) \quad \text{for } n \geq 1. \end{array} \tag{20}$$

For the particular experiments presented here we took $L = 0.1\hat{a}$ where $\hat{a}$ is the operator, which in the eigenbasis of H_f assumes the off-diagonal form

$$\begin{bmatrix} 0 & 1 & 0 & 0 & 0 & \dots \\ 0 & 0 & \sqrt{2} & 0 & 0 & \dots \\ 0 & 0 & 0 & \sqrt{3} & 0 & \dots \\ \vdots & \vdots & \vdots & \vdots & \vdots & \vdots \end{bmatrix} \tag{21}$$

The basis states are in order of increasing energy, with basis states in the degenerate subspaces listed in a particular order. The effect of this H_f-dependent Lindblad operator, in isolation, would be to relax the system to the selected ground state, thereby breaking the degeneracy. However, since it has a highly non-local action on the qubits, its interaction with $H(s)$ disturbs the adiabatic evolution and destroys the fine structure of the probability histogram. In this setting the probability of success is defined as $P = \mathrm{Tr}\left(\Pi\rho(1)\right)$ where, again, Π is the projector onto the ground state space of H_f. The range of computable systems appears bounded to 6 qubits and $T \approx 2.5$. Nevertheless within these bounds the method is fully reliable. Indeed, the test conducted in this regime with $L = 0$ gives results fully consistent with the pure Schrödinger, see Fig. 3.

C. Remarks about the efficiency of the numerical algorithms

–Conclusions.–

Our main motivation for this study has been the desire to better understand the mechanism behind the function of the D-Wave One quantum computer. To this end we undertook to develop an efficient numerical approach to simulations of quantum dynamics and to carry out a vast number of numerical experiments facilitating comparison between prediction of the quantum theory with the D-Wave one experiments reported in [1]. The proposed approach has made it possible for us to conduct numerical experiments with a substantial number of qubits and significant time scales for both non-dissipative and dissipative quantum dynamics. We have found that non-dissipative adiabatic evolution results in a multi-modal histogram of the probability of success, contrasting with a uni-modal histogram obtained in the presence of dissipation. Since the D-Wave One device (with any number of qubits between 8 and 108) displays a bi-modal histogram of the probability of success, our results indicate that its function may be modeled by Schrödinger, rather than master, equation. Moreover, the results we have obtained for the 12 qubit Schrödinger evolution confirm the existence of "hard cases" for which the probability of success falls very near 0, see Figs. 5, 6. This feature is also observed in D-Wave One histograms (see [1]). Although our computation times are several orders of magnitude shorter than the times used in D-Wave One, we are investigating smaller problem sizes and hence larger minimum gaps.

Acknowledgements. A.P.S. thanks the Department of Physics of the University of Loughborough for hosting him in the autumn of 2013 and acknowledges the support of the Canadian Foundation for Innovation, grant LOF # 22117. The authors are grateful to the referee for a prudent review, many thoughtful remarks and, particularly, for the challenge to come clear on the issue of true effectiveness of the proposed algorithm, which resulted in the development of material now included with the supplementary materials, part B.

[1] S. Boixo, T. F. Rønnow, S. V. Isakov, Z. Wang, D. Wecker, D. A. Lidar, J. M. Martinis, and M. Troyer (2013), arXiv:1304.4595, URL http://arxiv.org/abs/ 1304.4595.
[2] T.F. Rønnow et al., arXiv:1401.2910 (2014)
[3] Z. Bian et al., Phys. Rev. Lett. **111**, 130505 (2013)
[4] J.A. Smolin and G. Smith, arXiv:1305.4904 (2013)
[5] L. Wang et al., arXiv:1305.5837 (2013)
[6] S.W. Shin et al., arXiv:1401.7087 (2014)
[7] M.W. Johnson et al., Nature **473**, 194 (2011)
[8] R. Feynman, Int. J. Theor. Phys. **21**, 467 (1982)
[9] E. Farhi, J. Goldstone, S, Gutmann, J. Lapan, A. Lundgren, D. Preda, Science **292** (2001), 472–476
[10] M Cullimore, M J Everitt, M A Ormerod, J H Samson, R D Wilson and A M Zagoskin, J. Phys. A: Math. Theor. **45** 505305 (2012)
[11] I. Percival, Quantum State Diffusion, Cambridge University Press, Cambridge, UK, 1998
[12] M.S. Sarandy and D.A. Lidar, Phys. Rev. Lett. **95**, 250503 (2005)
[13] F. Barahona, J. Phys. A: Math. Theor. **15** (1982), 3241–3253

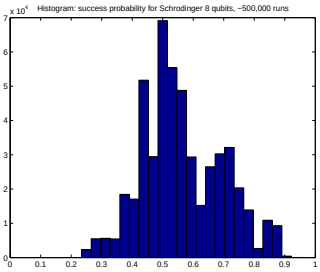

Figure 1. Results obtained via computation of Taylor series solutions of the 8 qubit adiabatic Schrödinger equation with $T = 4$. The histogram displays probability of success outcomes for $500,000$ random Ising Hamiltonians H_f sorted into 32 bins. The computation of these results took about 15 minutes on a cluster of 128 MATLAB "labs".

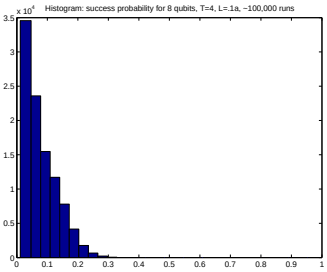

Figure 2. Results obtained via computation of Taylor series solutions of the 8 qubit master equation with the Lindblad operator $L = 0.1\hat{a}$ and $T = 4$. The probabilities of success outcomes obtained for $100,000$ random Ising Hamiltonians H_f are sorted into 32 bins. The computation of these results took about 45 hours on a cluster of 128 MATLAB "labs".

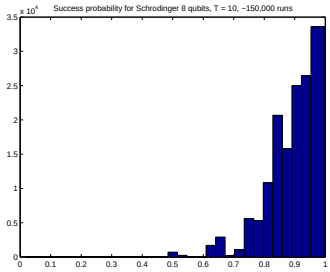

Figure 3. Schrödinger evolution as in Fig. 1 with 8 qubits but with $T = 10$. The histogram may be described as multi-modal.

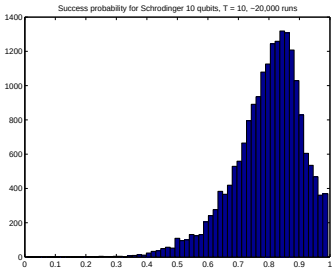

Figure 4. Schrödinger evolution as in Fig. 1 but with 10 qubits and $T = 10$. The histogram has 64 bins in order to emphasize multi-modality here visible as a barely visible island of results falling near .3.

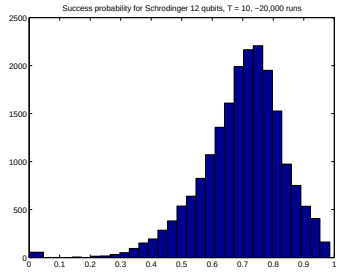

Figure 5. As in Fig. 1 but with 12 qubits and $T = 10$. Observe the presence of a small percentage of "hard cases" concentrating near zero, which amounts to multi-modality similar to that observed in D-Wave One experiments reported in [1]. The computation time was approximately 18 hours.

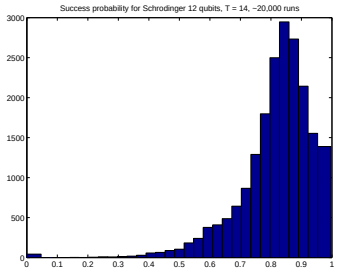

Figure 6. As in Fig. 1 but with 12 qubits and $T = 14$. As in Fig 5, one observes the presence of a small percentage of "hard cases" concentrating near zero. The computation time was approximately 18 hours.

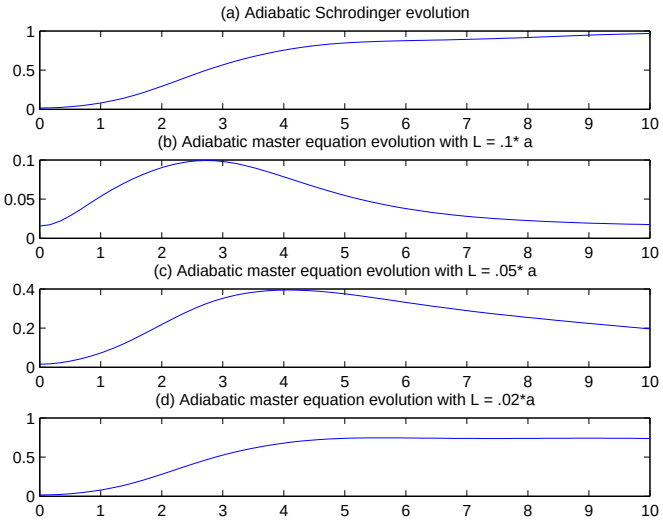

Figure 7. Dependence of the probability of success on T for solutions of the 8 qubit Schrödinger equation (a) and the master equations with the Lindblad operators $L = 0.1\hat{a}$ (b), $L = 0.05\hat{a}$ (c), and $L = 0.02\hat{a}$ (d). Note the inapplicability of the adiabatic theorem in (b) and (c), as well as convergence to the Schrödinger solution for diminishing norm of L.